Transitions in cell potency during early mouse development are driven by Notch

Sergio Menchero [1], Isabel Rollan [1], Antonio Lopez-Izquierdo [1], Maria Jose Andreu [1], Julio Sainz de Aja [1,2]

*For correspondence: mmanzanares@cnic.es

Present address: [2] Stem Cell Program, Boston Children's Hospital, Boston, United States; [3] The Francis Crick Institute, London, United Kingdom

Competing interests: The authors declare that no competing interests exist.

Funding: See page 23

Received: 17 October 2018
Accepted: 07 April 2019
Published: 08 April 2019

Reviewing editor: Elizabeth Robertson, University of Oxford, United Kingdom

eLife digest We start life as a single cell, which immediately begins to divide to form an embryo that will eventually contain all the different kinds of cells found in the adult body. During the first few

Once the embryo compacts, differences in cell membrane contractility and the activity of signalling pathways orchestrate the lineage-commitment of cell populations (Kono et al., 2014 ; Korotkevich et al., 2017 ; MaõÃtre et al., 2016; MihajlovicÂand Bruce, 2016 ; Nishioka et al., 2009 ; Nissen et al., 2017 ; Rayon et al., 2014). The initial stochastic expression of the main lineage-specific transcription factors (such as CDX2 or GATA3 for the TE, and OCT4 or NANOG for the ICM) is gradually restricted to their definitive domains (Dietrich and Hiiragi, 2007 ; Posfai et al., 2017). The Hippo pathway has been shown to act as a readout of cell polarity and therefore, differential intercellular distribution of its components and thus differential activity in polar or apolar cells, will dictate fate (Cockburn et al., 2013 ; Hirate et al., 2013 ; Leung and Zernicka-Goetz, 2013 ; Wicklow et al., 2014). In outer cells, the pathway is switched off and the transcriptional coactivator YAP is translocated to the nucleus where it will interact with TEAD4, the effector of the pathway, to promote the expression of key TE genes such as *Cdx2* and *Gata3* (Nishioka et al., 2009 ; Ralston et al., 2010). We have previously shown that Notch signalling also has a role in the regulation of *Cdx2*. It is specifically active in the TE, where the intracellular domain of the Notch receptor (NICD) is translocated into the nucleus where it binds to the transcription factor RBPJ to promote target gene expression. Both Notch and Hippo converge on the TEE, an enhancer upstream of *Cdx2* (Rayon et al., 2014). YAP/TEAD and NICD/RBPJ transcriptional complexes interact with the chromatin modifier SBNO1 to favour the induction of *Cdx2* (Watanabe et al., 2017).

Nevertheless, we still do not understand how these two signalling pathways interact to regulate Cdx2 in the embryo, if there is crosstalk between them, if they are acting in parallel during development or otherwise. Furthermore, Notch signalling could have other unexplored roles at early stages of mouse development. In this study, we show that Hippo and Notch pathways are largely independent, but that Notch is active earlier, before compaction, and that differences in Notch levels contribute to cell fate acquisition in the blastocyst. Single-embryo RNA-seq points at repressors that block early naÈve pluripotency markers as Notch targets. We propose that Notch coordinates the

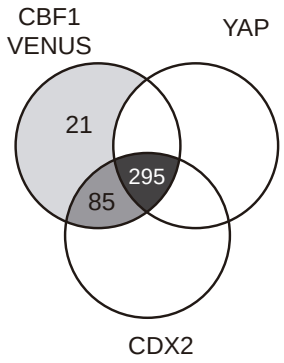
CBF1
VENUS
YAP
21
295
85
CDX2

regulate Cdx2 levels in a stage specific manner rather than being redundant. Interestingly, Gata3, a known target of YAP-TEAD4 independent of Cdx2 (Ralston et al., 2010) is downregulated by Verteporfin in embryos treated from the two-cell to morula stage (Figure 1A). This suggests that certainly Hippo signalling acts differently on its various targets, as are Cdx2 or Gata3. Oct4 and Nanog were not significantly changed after Notch or YAP inhibition in any of the time windows.

Next, we wished to confirm these observations in morula stage embryos using genetic loss of function models. We recovered early (8±16 cells) and late (17±32 cells) morulae and analysed CDX2 expression in wildtype and $Rbpj^{-/-}$ embryos (Figure 2C±E). We found that $Rbpj^{-/-}$ early morulae had

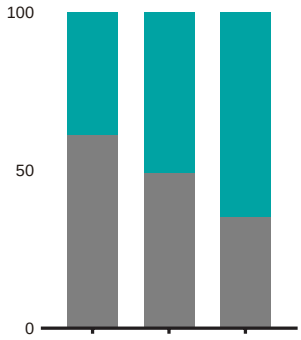
100
50
0

their descendant cells. We next classified families according to the position of the cells in the first and final time points. This allowed us to divide the cells in four groups: `IN-ICM' (cells that began in an inner position and their descendants remained in an inner position), `IN-TE +ICM' (cells that began in an inner position and at least one of their descendants ended up in an inner position but

this effect and whether blocking Notch would have an effect in early embryos. To address these questions, we used a genetic mosaic line (iChr-Notch-Mosaic) that allowed us to generate cells with different Notch activity levels within the same embryo (Pontes-Quero et al., 2017). The construct consists of three different cassettes preceded by a specific LoxP site. The first cassette is a H2B-CHERRY fluorescent protein and generates wildtype cells. The second cassette contains a dominant-negative version of Mastermind-like 1 (DN-MAML1), a transcriptional co-activator of the Notch pathway, linked to a H2B-eGFP by a cleavable 2A peptide, whose expression leads to the loss of function (LOF) of the pathway, while the third is a gain of function (GOF) cassette through the expression of a constitutively active NICD linked to an HA-H2B-Cerulean (Figure 4A). The specific LoxP sites are mutually exclusive, so in any unique cell there will be only one possible outcome as the result of Cre-mediated recombination. We used a Polr2a^{CreERT2} driver which is ubiquitously expressed and inducible by tamoxifen (Guerra et al., 2003). We induced recombination by adding 4OH-Tx (4-hydroxy-tamoxifen) from the 2- to the 4-cell stage, aiming to achieve a situation where cells expressing each cassette derive from a single recom-

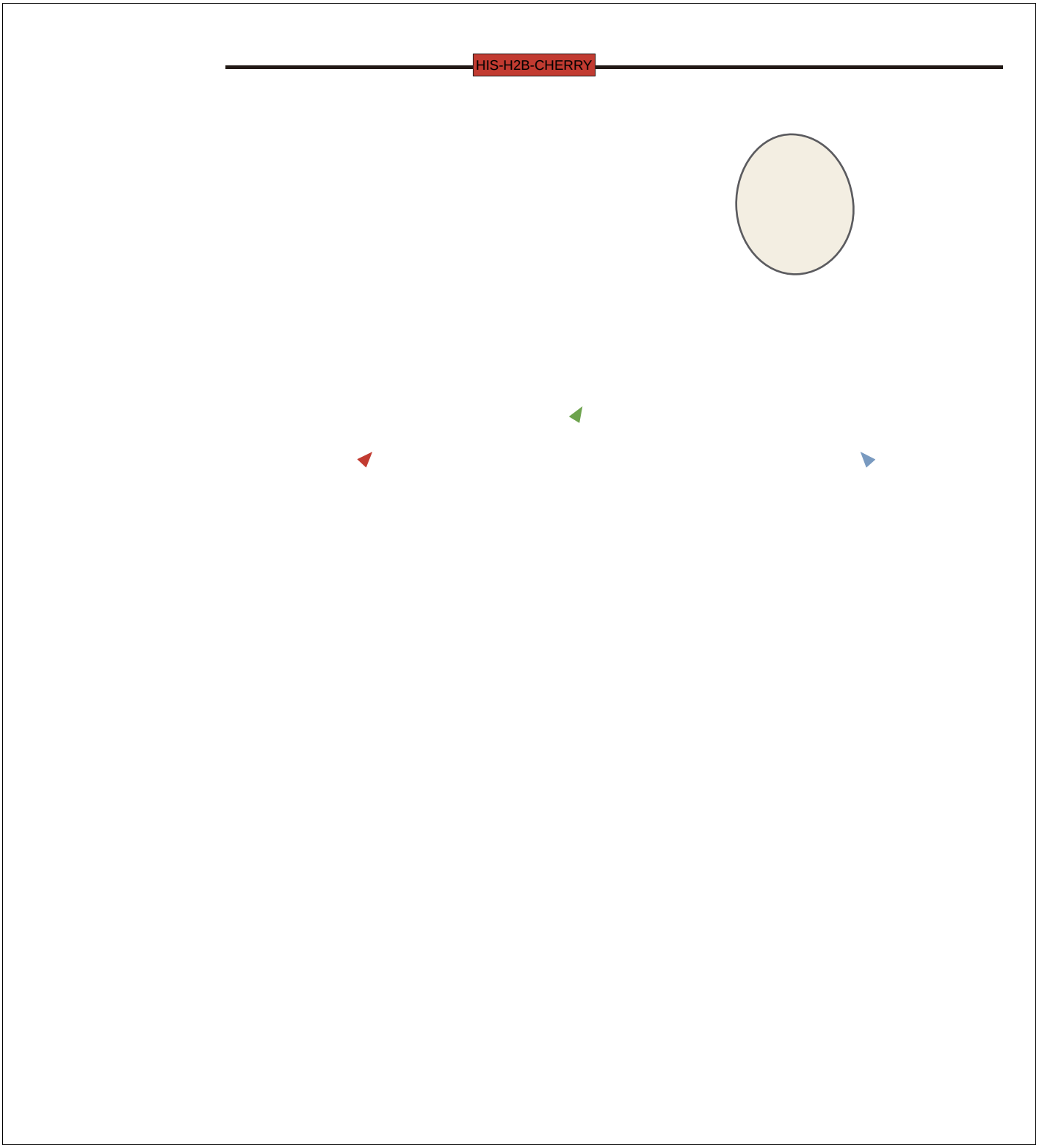
HIS-H2B-CHERRY

Lack of Rbpj represses Tle4 and Tbx3, and disrupts the triggering of differentiation programs in the early embryo

Results described above show that the Notch pathway plays an early role in mouse development, non-redundant with that of the Hippo pathway, in regulating Cdx2 gene expression and in determin-

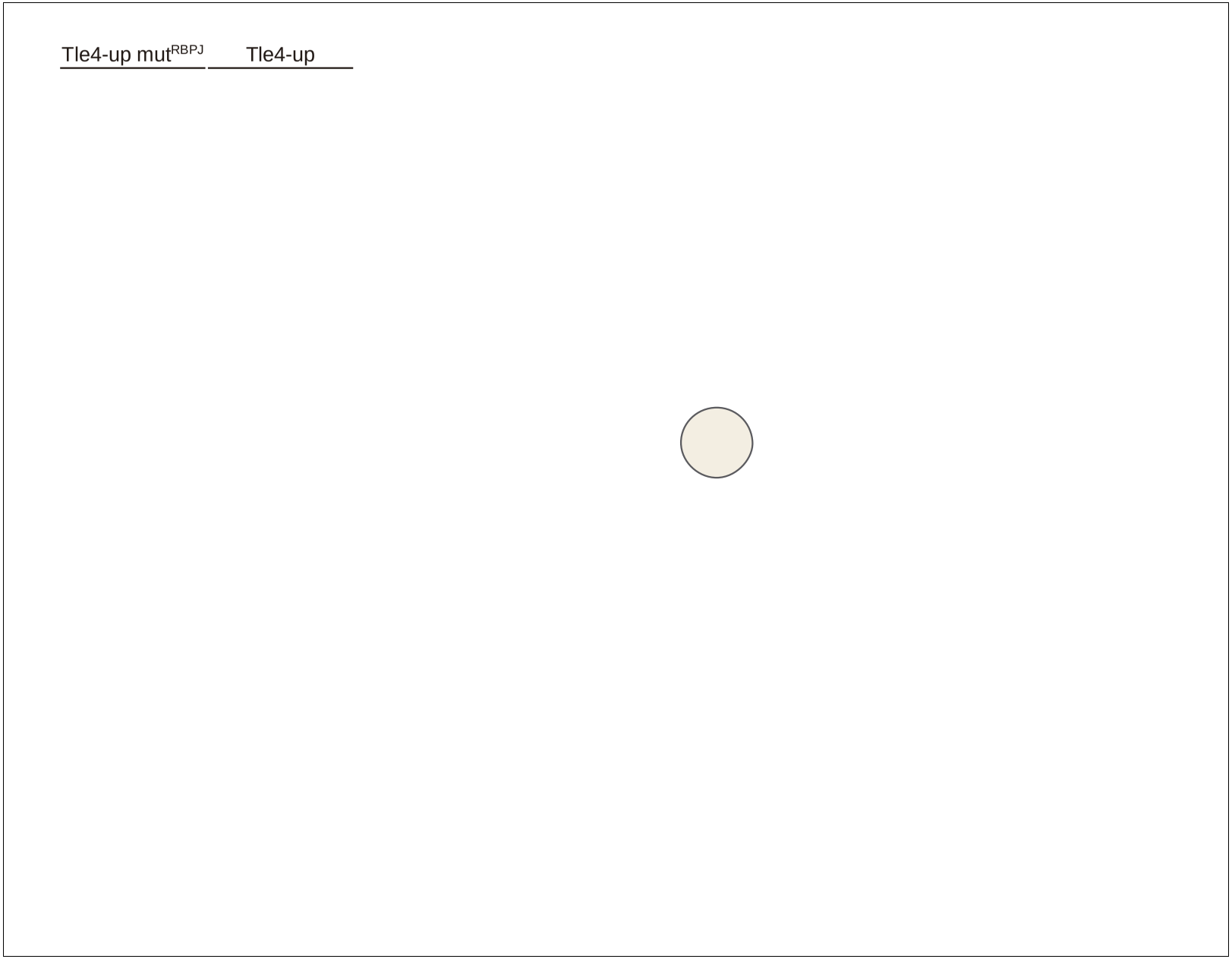
Tle4-up mut^RBPJ
Tle4-up

their expression after blocking the Notch pathway by treating wildtype embryos with the RO4929097 inhibitor from 2 cell to morula stage (Figure 5C).

An RBPJ motif search within ATAC-seq peaks in the vicinity of the genes identified two potential candidate regions located 1.3 Kb upstream of Tle4 (Tle4-up; Figure 5D) and in the seventh intron of Tbx3 (Tbx3-i7; Figure 5Ðfigure supplement 2A), respectively. By means of transient transgenic assays(Rayon et al., 2014

Analysis of published single-cell RNA-seq data (Goolam et al., 2016) confirmed that Prdm14 decreased dramatically from the 4- to 8-cell stage, and expression of Dppa3 also decreases from the 2- to the 4-cell stage (Figure 6Ðfigure supplement 1). In contrast, Tle4 and Tbx3 levels increased from the 4- to 8-cell stage (Figure 6Ðfigure supplement 1). Our data from Rbpj$^{-/-}$ morulae suggests that suggests

-294.1-592.10Tj 1 0 0 1 468.283 731.679 Tm -a966781_2 8.96,0 12.13ppa3whos.001031 0 Td -367.9 12.108 Tdwe 131.00e55 0 signif-29nt.597.00e22532

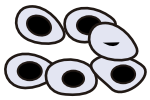

simply turning off the general pluripotency network to promote differentiation, but acting on a subset of early naïve pluripotency markers.

Interplay between Notch and chromatin remodellers has been reported in several situations (Schwanbeck, 2015). Expression changes in chromatin modifiers precede the action of transcription factors that consolidate lineage choices during preimplantation development (Burton et al., 2013). Therefore, these alterations suggest that Rbpj$^{-/-}$ embryos do not established correct epigenetic landscapes, do not switch off early markers such as Prdm14 or Dppa3 and are not able to properly trigger differentiation programs leading to a delay in the expression of lineage specifiers such as Cdx2. In this regard, it is interesting to note that Rbpj mutant morulae downregulate Chaf1a, which encodes the large subunit of the histone-chaperone CAF-1. Loss of CAF-1 promotes ES cells to transit to an earlier, totipotent 2-cell-like state (Ishiuchi et al., 2015), and acts as a barrier for reprogramming (Cheloufi et al., 2015). Furthermore, knockout of Chaf1a leads to developmental arrest at the 16-cell stage and a loss of heterochromatin (Houlard et al., 2006). Thus, CAF-1 acts as a driver of differentiation in pluripotent cells. Interestingly, studies in Drosophila have shown that CAF-1 mediates downstream effect of the Notch pathway (Yu et al., 2013). On the other hand, Asf1a, which encodes another histone chaperone, is among the few genes observed to be upregulated in Rbpj$^{-/-}$ embryos. Forced expression of Asf1a promotes reprogramming of human ES cells (Gonzalez-MunÄoz

Continued

Reagent type (species) or resource	Designation	Source or reference	Identifiers	Additional information
Strain (Mus musculus)	CD1	Charles Rivers		
Strain (Mus musculus)	C57Bl/6	Charles Rivers		
Strain (Mus musculus)	CBA	Charles Rivers		
Genetic reagent (M. musculus)	CBF1-VENUS	Nowotschin et al., 2013	MGI:5487911	Dr. Anna-Katerina Hadjantonakis
Genetic reagent (M. musculus)	Rbpj null	Oka et al., 1995	MGI:1857411	Dr. Jose Luis de la Pompa
Genetic reagent (M. musculus)	Notch1 null	Conlon et al., 1995	MGI:1857230	Dr. Jose Luis de la Pompa
Genetic reagent (M. musculus)	Tead4 null	Nishioka et al., 2008	MGI:3770620	Dr. Hiroshi Sasaki
Genetic reagent (M. musculus)	iChr-Control-Mosaic	Pontes-Quero et al., 2017	MGI:6108166	Dr. Rui Benedito
Genetic reagent (M. musculus)	iChr-Notch-Mosaic	Pontes-Quero et al., 2017		Dr. Rui Benedito
Genetic reagent (M. musculus)	Polr2a-CreERT2	Guerra et al., 2003	MGI:3772332	Dr. Miguel Torres
Cell				

Continued

Reagent type (species) or resource	Designation	Source or reference	Identifiers	Additional information
Sequence-based reagent	qPCR primers	This paper		See Supplementary file 1
Commercial assayor kit	PicoPure RNA Isolation Kit	ThermoFisher	KIT0204	
Chemical compound, drug	RO4929097	Selleckchem	S1575	
Chemical compound, drug	Verteporfin	Sigma	SML0534	
Software, algorithm	MINS	Lou et al., 2014		
Software, algorithm	GraphPad Prism	www.graphpad.com	RRIDSCR_015807	
Software, algorithm	Fiji	fiji.sc	RRIDSCR_002285	
Software, algorithm	R Project for Statistical Computing	www.r-project.org	RRIDSCR_001905	

Animal experimentation

The following mouse lines were used in this work: CBF1-VENUS(Nowotschin et al., 2013), Rbpj null (Oka et al., 1995), Tead4 null (Nishioka et al., 2008), Notch1 null (Conlon et al., 1995), iChr-Notch-Mosaic (Pontes-Quero et al., 2017), iChr-Control-Mosaic (Pontes-Quero et al., 2017), Polr2a^{CreERT2} (Guerra et al., 2003). All the lines were maintained in heterozygosis in an outbred background.

7.90(r7oterozygosis)-4628-458Sed0pd(R96Adults were(the)-457.816(lines)Tj 14rk:)]Tly5458.966 T(c7v.285crib9668swhr)0.9-58 7.97 Tf -217.531 -239l1toz

were used for imaging each experiment. Semi-automated 3D nuclear segmentation for quantification of fluorescence intensity was carried out using MINS, a MATLAB-based algorithm (http://katlab-tools.org/) (Lou et al., 2014), and analysed as previously described (Saiz et al., 2016). To correct z-associated attenuation, intensity levels were fit to a linear model. Mitotic and pyknotic nuclei were excluded from the analysis. For defining cells as positive or negative for a given nuclear marker, we ordered cells by intensity levels and established a threshold for each experiment based on manual verification of the point where nuclear and cytoplasmic signals were equal. This process was repeated independently for each set of embryos processed and imaged in parallel, to overcome inter-experimental variability.

For live imaging, embryos were cultured in microdrops of KSOM on glass-bottomed dishes (MatTek) in an environmental chamber as described previously (Xenopoulos et al., 2015). Images were acquired with a Zeiss LSM880 laser scanning confocal microscope system using a 40x objective. An optical section interval of 1.5 mm was acquired per z-stack, every 15 min.

Cell tracking of 3D-movies was carried out using a TrackMate plugin in Fiji (FernaÂndez-de-ManuÂel et al., 2017; Schindelin et al., 2012 ; Tinevez et al., 2017). The 3D reconstruction of the embryos and position of the cells was done using MatLab. The shape of the embryos was fitted into an ellipse and the coordinates in X, Y, Z for each blastomere were normalised to the centroid of the ellipse. The algorithm assigned an inner or outer position to each blastomere according to an established threshold, and they were manually verified. The intensity levels of VENUS fluorescent protein in each cell and time point were normalised according to the Z-position to correct the decay of signal intensity due to the distance with the objective (Saiz et al., 2016). The frequencies of the intensity levels for each embryo followed a Gaussian distribution. In order to compare different embryos, intensity levels were normalised so that the mean was 0 and the standard deviation was 1.

Pharmacological inhibitor treatments

Two-cell or morula stage embryos were cultured in drops of M16 medium (Sigma) covered with mineral oil (NidOil, EMB) at 37 ÊC, 5% CO_2, containing the corresponding pharmacological inhibitor or only DMSO as control until the corresponding stage. The following inhibitors and concentrations were used: 10 or 20 mM of the g-secretase inhibitor RO4929097 (S1575, Selleckchem) (Mu¨nch et al., 2013) and 10 mM of the TEAD/YAP inhibitor Verteporfin (SML0534, Sigma) (Liu-Chittenden et al., 2012).

Quantitative-PCR

RNA from pools of 25±30 embryos (for pharmacological inhibitor experiments) or from single embryos (for CRISPR/Cas9 editing) was isolated using the Arcturus PicoPure RNA Isolation Kit (Applied Biosystems) and reverse transcribed using the Quantitect Kit (Qiagen). RNA was isolated from ES cells with the RNeasy Mini Kit (Qiagen) and reverse transcribed using the High Capacity cDNA Reverse Transcription Kit (Applied Biosystems). cDNA was used for quantitative-PCR (qPCR) with Power SYBR Green (Applied Biosystems) in a 7900HT Fast Real-Time PCR System (Applied Biosystems). Expression of each gene was normalized to the expression of the housekeeping genes Actin (in mESC or pools of embryos) or 18S rRNA (in single embryos). Primers used are detailed in Supplementary file 1 .

RNA-sequencing data analysis

RNA-seq was performed on single morulae. cDNA synthesis was performed using SMART-Seq Ultra Low Input RNA Kit (Clontech). Library preparation and sequencing was performed by the CNIC Genomics Unit using the Illumina HiSeq 2500 sequencer. Gene expression analysis was performed by the CNIC Bioinformatics Unit. Reads were mapped against the mouse transcriptome (GRCm38 assembly, Ensembl release 76) and quantified using RSEM v1.2.20 (Li and Dewey, 2011). Raw expression counts were then processed with an analysis pipeline that used Bioconductor packages EdgeR (Robinson et al., 2010) for normalisation (using TMM method) and differential expression testing. Expression data of Rbpj and Neo were used to genotype the samples. Three mutant and three control (two wildtype and one heterozygote) embryos were selected for analysis. Changes in gene expression were considered significant if associated to Benjamini and Hochberg adjusted p-value<0.05.

(Hyclone), 0.1% û-mercaptoethanol (Sigma) and LIF (produced in-house) or 2i (CHIR-99021, Selleckchem; and PD0325901, Axon) in dishes seeded with a feeder layer of mouse embryonic fibroblasts (MEFs). Cells were transfected with a Cre expressing plasmid to induce recombination using Lipofectamine 2000 (Invitrogen) for 24 hr. After recombination, cells were sorted using a Becton Dickinson FACS Aria Cell Sorter. To promote spontaneous differentiation, cells were cultured on gelatine-covered dishes for 48±72 hr afters0]TJ 339.o82 (ptJ.004339.o82-327.606 (z4pe1amoov7 8.96.e1am0ot2fAF262

Ministerio de Economía y Competitividad	SEV-2015-0505	Sergio Menchero Isabel Rollan Antonio Lopez-Izquierdo Maria Jose Andreu Julio Sainz de Aja Javier Adan Rui Benedito Teresa Rayon Miguel Manzanares
Ministerio de Economía y Competitividad	SVP-2013-067930	Sergio Menchero
National Institutes of Health	NIH-R01HD094868	Minjung Kang Anna-Katerina Hadjantonakis
National Institutes of Health	NIH-P30CA008748	Minjung Kang Anna-Katerina Hadjantonakis

The funders had no role in study design, data collection and interpretation, or the decision to submit the work for publication.

Author contributions

Sergio Menchero, Conceptualization, Data curation, Software, Formal analysis, Validation, Investigation, Visualization, Methodology, WritingÐoriginal draft, Project administration, WritingÐreview and editing; Isabel Rollan, Investigation, Methodology, WritingÐreview and editing; Antonio Lopez-Izquierdo, Data curation, Software, Formal analysis, Investigation, Visualization, Methodology, WritingÐreview and editing; Maria Jose Andreu, Javier Adan, Investigation, WritingÐreview and editing; Julio Sainz de Aja, Formal analysis, Investigation, WritingÐreview and editing; Minjung Kang, Data curation, Investigation, WritingÐreview and editing; Rui Benedito, Resources, WritingÐreview and editing; Teresa Rayon, Conceptualization, WritingÐreview and editing; Anna-Katerina Hadjantonakis, Conceptualization, Resources, Funding acquisition, WritingÐreview and editing; Miguel Manzanares, Conceptualization, Supervision, Funding acquisition, Validation, WritingÐoriginal draft, Project administration, WritingÐreview and editing

Author ORCIDs

Sergio Menchero

Grabole N , Tischler J, Hackett JA, Kim S, Tang F, Leitch HG, Magnúsdóttir E, Surani MA. 2013. Prdm14

Laing AF, Lowell S, Brickman JM. 2015. Gro/TLE enables embryonic stem cell differentiation by repressing pluripoten t gene expression. Developmental Biology 397:56±66. DOI: https://doi.org/10.1016/j.ydbio.2014.10.007, PMID: 25446531

Leung CY, Zernicka-Goetz M. 2013. Angiomotin prevents pluripotent lineage differentiation in mouse embryos via hippo pathway-dependent and -independent mechanisms. Nature Communications 4:2251. DOI: https://doi.org/1 0.1038/ncomms3251, PMID: 23903990

Posfai E, Petropoulos S, de Barros FRO, Schell JP, Jurisica I, Sandberg R, Lanner F, Rossant J. 2017. Position- and hippo signaling-dependent plasticity during lineage segregation in the early mouse embryo. eLife 6: e22906. DOI: https://doi.org/10.7554/eLife.22906 , PMID: 28226240

Quinlan AR , Hall IM. 2010. BEDTools: a flexible suite of utilities for comparing genomic features. Bioinformati cs 26:841±842. DOI: https://doi.org/10.1093/bioinformatics/btq033 , PMID: 20110278

Ralston A , Cox BJ, Nishioka N, Sasaki H, Chea E, Rugg-Gunn P, Guo G, Robson P, Draper JS, Rossant J. 2010. Gata3 regulates trophoblast development downstream of Tead4 and in parallel to Cdx2. Development 137: 395±403. DOI: https://doi.org/10.1242/dev.038828 , PMID: 20081188

Ralston A , Rossant J. 2008. Cdx2 acts downstream of cell polarization to cell-autonomously promote trophec toderm fate in the early mouse embryo. Developmental Biology 313:614±629. DOI: https://doi.org/10. 1016/j.yd bio.2007.10.054 , PMID: 18067887

Ran FA, Hsu PD, Wright J, Agarwala V, Scott DA, Zhang F. 2013. Genome engineering using the CRISPR-Cas9 system. Nature Protocols 8:2281±2308. DOI: https://doi.org/10.1038/nprot.2013.143 , PMID: 24157548

Rayon T, Menchero S, Nieto A, Xenopoulos P, Crespo M, Cockburn K, CanÄon S, Sasaki H, Hadjantonakis AK, de la Pompa JL, Rossant J, Manzanares M. 2014. Notch and hippo converge on Cdx2 to specify the trophectoderm lineage in the mouse blastocyst. Developmental Cell 30:410±422. DOI: https://doi.org/10.1016/ j.devcel.2014.06.019, PMID: 25127056

Robinson MD, McCarthy DJ, Smyth GK. 2010. edgeR: a bioconductor package for differential expression analysis of digital gene expression data. Bioinformatics 26:139±140. DOI: https://doi.org/10.1093/bioinformatics/ btp616 , PMID: 19910308

Russell R, Ilg M, Lin Q, Wu G, Lechel A, Bergmann W, Eiseler T, Linta L, Kumar P P, Klingenstein M, Adachi K, Hohwiel er M, Sakk O, Raab S, Moon A, Zenke M, Seufferlein T, Schë er HR, Illing A, Liebau S, et al. 2015. A dynamic role of TBX3 in the pluripotency circuitry. Stem Cell Reports 5:1155±1170. DOI: https://doi.org/10. 1016/j.stemcr.2015.11.003, PMID: 26651606

Saiz N, Kang M, Schrode N, Lou X, Hadjantonakis A-K. 2016. Quantitative analysis of protein expression to study lineage specification in mouse preimplantation embryos. Journal of Visualized Experiments 108:e53654. DOI: https://doi.org/10.3791/53654

Sasaki H. 2015. Position- and polarity-dependent hippo signaling regulates cell fates in preimplantation mouse embryos. Seminars in Cell & Developmental Biology 47-48:80±87. DOI: https://doi.org/10.1016/j.semcdb.2015. 05.003, PMID: 25986053

Schindelin J , Arganda-Carreras I, Frise E, Kaynig V, Longair M, Pietzsch T, Preibisch S, Rueden C, Saalfeld S, Schmid B, Tinevez JY, White DJ, Hartenstein V, Eliceiri K, Tomancak P, Cardona A. 2012. Fiji: an open-source , PMID: 33°53

Wennekamp S, Mesecke S, Nédélec F, Hiiragi T. 2013. A self-organization framework for symmetry breaking in the